https://doi.org/10.5194/egusphere-2025-1254
Preprint. Discussion started: 5 May 2025

Hillslope subsurface flow is driven by vegetation more than soil properties in colonized valley moraines along a humid mountain elevation

Fei Wang[1,2], Genxu Wang[3], Junfang Cui[4], Xiangyu Tang[5], Ruxin Yang[6], Kewei Huang[7], Jianqing Du[2], Li Guo[3]

[1]College of Resources and Environment, University of Chinese Academy of Sciences, Beijing 100049, China
[2]Beijing Yanshan Earth Critical Zone National Research Station, University of Chinese Academy of Sciences, Beijing 101408, China
[3]State Key Laboratory of Hydraulics and Mountain River Engineering, College of Water Resource and Hydropower, Sichuan University, Chengdu 610065, China
[4]Institute of Mountain Hazards and Environment, Chinese Academy of Sciences, Chengdu 610299, China
[5]State Key Laboratory of Subtropical Silviculture, Zhejiang A&F University, Hangzhou 311300, China
[6]School of Environmental Science and Engineering, Southwest Jiaotong University, Chengdu 610031, China
[7]Hubei Key Laboratory of Basin Water Security, Changjiang Institute of Survey, Planning, Design and Research, Wuhan 430010, China

Correspondence to: Genxu Wang (wanggx@scu.edu.cn) and Li Guo (liguo01@scu.edu.cn)

Abstract. Valley moraines along an elevation gradient are colonized by different climax vegetation, where preferential flow paths (PFPs) and ground layer, as important hillslope structures, significantly influence hillslope flow. However, the roles of these hillslope structures in flow dynamics and the underlying mechanisms in contrasting ultimate forests within moraines remains enigmatic. To this end, we conceptualized PFPs and the ground layer as explicit elements in the HYDRUS 2D, constructing set-ups of hillslope internal structures that incorporate an optional ground layer and varying intensities of PFPs using the random placement method to represent the shallow root zone (0-50 cm) of vegetated moraines. The results showed that, out of the 50 set-ups in each forest type, only 3 set-ups in the coniferous forest and 2 set-ups in the broadleaf forest successfully predicted the dynamics and water balance of the hydrological response at the event scale. Notably, all 5 successful set-ups featured below-average vertically connected PFPs that were only 5% of total spatial area in both forests, following the principle of maximum free energy dissipation, which is achieved when flow passes through a network composed of partial PFPs and steepened soil matrix gradient. The similar percentage of PFPs between forest types is attributed to similar coarse-textured soils, which resulted from frequent precipitation and clay washout, as well as comparable fine root in both forests. In addition, a linear relationship between vertical PFPs and hillslope flow was observed in both forests, with the coniferous forest being more sensitive to changes in the vertical PFPs due to lower soil organic matter. The presence of ground layer caused the PFPs to be buried, reduced the exchange between PFPs and soil matrix due to fast lateral flow towards downslope within the ground layer, leading to earlier peak flow timing and increased peak flow. This study highlights the roles of the ground layer and the fine root from vegetation in influencing subsurface flow, advancing our understanding of hillslope structures and runoff evolution over time in humid valley moraines.

https://doi.org/10.5194/egusphere-2025-1254
Preprint. Discussion started: 5 May 2025

1 Introduction

Hillslope as the basic functional component of catchment exerts a dominant impact on the hydrological responses of stream water (Anderson et al., 2009; Angermann et al., 2017; Hartmann and Blume, 2024). The hydrological responses of hillslope depend on the hillslope/soil structure, which is in determination of soil water dynamics, subsurface flow paths, and flow fluxes (Hartmann et al., 2020b; Wienhöfer et al., 2009; Jackisch et al., 2017; Jarvis et al., 2024). Structural features, such as macropores formed by roots, soil fauna, and fractures, or soil cracks serve as effective and efficient means for in situ determination of hillslope/soil structures and flow dynamics (Graham and Lin, 2012; Beven and Germann, 2013; Uchida et al., 2002; Cheng et al., 2017; Jackisch et al., 2017).

Flow through preferred paths with velocities and fluxes orders of magnitude greater than flow through the soil matrix, bypassing a large fraction of soil matrix, is preferential flow. Preferential flow and associated preferential flow paths (PFPs) have been proved to be the rule rather than the exception in the field (Jarvis, 2007; Beven and Germann, 2013; Jarvis et al., 2016). This ubiquitous phenomenon (i.e., preferential flow in soil) can be understood from a thermodynamic perspective(Lin, 2010), where water flow tends to minimize resistance, thereby enabling a more efficient redistribution of water. Obviously, water flow through PFPs adheres to the principle of minimizing resistance, primarily caused by friction and capillary force, which explained the prevalence of preferential flow across different soil types. This behaviour probably also underlines the evidence that only a small fraction of PFPs is actively involved in water movement, yet they are responsible for a substantial portion of water transport across various soil types. The phenomenon, primarily attributed to isolated PFPs that disconnected from flow network or to air entrapment during infiltration (Jarvis et al., 2016), has been observed in various soils, including agricultural silt loam (Luo et al., 2008), grassy coarse sandy loam (SněHota et al., 2010), silty clay soil developed from postglacial lake sediment (Koestel and Larsbo, 2014), and cultivated silt clay loam developed from Loess (Sammartino et al., 2015). Additionally, it has also been observed in connected PFPs, which are considered the dominant continuum for water flow in heterogeneous soils. Koestel and Larsbo (2014) identified that solute transport predominantly occurred through two cylindrical PFPs. Similarly, Sammartino et al. (2015) showed that a single dominant flow network, largely composed of the active macropores fraction, was responsible for water flow. While, how vegetation and soil type influence the PFPs involved in water flow, as well as the underlying causes, remain questions yet to be explored.

In alpine mountains, deposited moraines resulting from widespread glacier retreat since Holocene experienced successive colonization of vegetation. As the climax vegetation (ultimately deciduous or evergreen trees) is succeed that endures indefinitely in moraines, the soil, particularly the shallow soil where roots are concentrated, is in equilibrium with prevailing environmental conditions (Huggett, 1998; Hartmann and Blume, 2024). This provided an ideal platform to investigate the intricate interactions between environment, vegetation, soil macropores, and the associated runoff processes. Vegetation colonization results in two distinct features: ground layer generation and soil formation processes (Hartmann et al., 2022; Laine-Kaulio et al., 2015; Hartmann et al., 2020b). Ground layer has the capability of intercepting falling rainfall (Zhu et al., 2020) and disconnecting the PFPs with soil surface. The former function determined the net amount of rainfall input and

https://doi.org/10.5194/egusphere-2025-1254
Preprint. Discussion started: 5 May 2025

arrival time of rainfall into soils , thereby posing significant influence on hydrological processes such as runoff generation, peak flow, and peak flow timing (Gomyo and Kuraji, 2016). The latter function is akin to tillage soil, where transport processes above the plough pan are partly disrupted due to the burial of PFPs during tillage operation (Akay and Fox, 2007; Bogner et al., 2013). Many studies have been focused on ground litter interception capacity, such as maximum storage and minimum storage (Guevara-Escobar et al., 2007; Li et al., 2017), ignoring its role of disconnecting macropores from soil surface. As to soil formation processes, particularly the development of soil structures, significant alterations were observed due to changes in the presence of PFPs, which are primarily in form of macropore channels created by activities of roots and soil fauna. These alterations in PFPs significantly played a crucial role in impacting both the surface and subsurface water flow. Studies on PFPs in glacial sandy till soils or vegetation-colonized moraines have been conducted in various regions (Laine-Kaulio et al., 2015; Hartmann and Blume, 2024); however, few have specifically focused on the PFPs involved in water transport. Advancing this research would certainly promote our understanding of the underlying mechanism and improve the accurate prediction of runoff processes with significant preferential flow in alpine mountains.

The methods employed to investigate PFPs involved in water flow include Computed Tomography (CT), Magnetic resonance imaging (MRI), positron emission tomography (PET), and numerical modelling, all of which require reconciling scales with study precision (Jarvis et al., 2016). Moreover, many of these methods are unable to applied to the forest ground layer due to its loose structure. The appropriate method accounting for the ground layer and PFPs is numerical models, in which PFPs and ground layer can be represented either implicitly or explicitly (Kirchner et al., 2023; Šimůnek et al., 2003; Rasoulzadeh and Homapoor Ghoorabjiri, 2013). Explicit models consider porous media as fine-scale elements to geometrically separate the PFPs from the soil matrix, providing an advantage in understanding the interplay between models output and structures. Despite the difficulty in acquiring detailed subsurface structures, previous studies have found it feasible to use random placement or genetic modelling of structures, with parameters derived from detailed plot-scale observations (Vogel et al., 2006; Weiler and Mcdonnell, 2007; Klaus and Zehe, 2011; Wienhöfer and Zehe, 2014). Furthermore, it enables us to evaluate the extent to which field evidence can effectively constrain and elucidate the role of PFPs in runoff processes.

In this study, we selected typical evergreen coniferous forest and deciduous broadleaf forest along an elevation gradient in a humid mountainous area, representing ultimate stages of vegetation colonization in the moraines. Broadleaf forest, situated at lower elevations with higher temperatures, accelerate moraine weathering, enhance organic matter decomposition and ground litter accumulation during soil formation processes, in contrast to coniferous forest at higher elevations. These processes enhance soil water-holding capacity and increase macropore formation. Meanwhile, the humid climate also controls initial wetness and hydraulic conductivity of soil and ground layer, leading to limited water deficit and fast water transport. Thus, we hypothesis that (1) forest ground layer significantly influence the outflow dynamics by disconnecting preferential flow than interception; (2) there is more PFPs involved in hillslope subsurface flow in the broadleaf forest due to increased biological activities at lower elevation; (3) the coniferous forest is less sensitive to changes in PFPs because of low soil water-holding capacity. To answer the questions, field and laboratory experiments on PFPs, soil properties, and ground

https://doi.org/10.5194/egusphere-2025-1254
Preprint. Discussion started: 5 May 2025

layer were conducted or collected, then represented explicitly in HYDRUS 2D to investigate the interplay between hillslope structures and subsurface flow over two colonized forests in moraines. The results of this study would guide our conceptualization of numerical model with field evidences to predict hillslope runoff, and promote our understanding of hydrological processes during moraines colonization and ongoing forest transformation under global climate change.

2 Materials and methods

2.1 Study sites description

2.1.1 Description of the valley moraines

Gongga mountain, located on the east edge of Tibetan Plateau, experienced extensive and repeated glaciation during the Quaternary glacial-interglacial cycles (Wang et al., 2012). Hailuo Valley, one of five distinctive sets of preserved moraines and associated glacial sediments in the Gongga mountain, features varying forest types along the retreat moraines due to dramatic elevation rise within a short horizontal distance. We selected two typical forest types in the Hailuo Valley: a coniferous forest at 3020 m a.s.l., developed from Neoglacial moraines, with *Abies fabri* and *Picea brachytyla* as climax vegetation; and a broadleaf forest at 2060 m a.s.l., developed from MIS2 moraines, with *Lithocarpus cleistocarpus* and *Cercidiphyllum japonicum* as climax vegetation (Hu et al., 2018; Wang et al., 2012). The soils in the two forests were classified as Cambisols based on IUSS working group WRB (2022). In the root zone (0–50 cm), soil in shallow layer (0–30 cm) is organic-rich with low bulk density (mean values of 0.82 g cm^{-3} in the coniferous forest and 0.78 g cm^{-3} in the broadleaf forest), and an increase in soil bulk density below 30 cm was found in both forests (0.98 g cm^{-3} and 1.15 g cm^{-3} in the coniferous and broadleaf forests, respectively). The mean sand content exceeded 85% in both forests, and the clay content was less than 4%, with no significant difference between forests. Additionally, both forests had a mean value of ~3 cm thick ground layer, consisting of a mixture of moss and litter in the coniferous forest and primarily litter in the broadleaf forest (Fig. S1). A higher root biomass, residual soil water content, and saturated soil hydraulic conductivity was observed in the broadleaf forest compared with that in the coniferous forest (Wang et al., 2022; Wang et al., 2023). The mean rock fragment content was 7.77 ± 2.54 cm^3 cm^{-3} in the coniferous forest and 6.50 ± 2.91 cm^3 cm^{-3} in the broadleaf forest, showing no difference between the forest types ($p > 0.05$).

2.1.2 Artificial field configuration

Field observation of the rainfall-runoff process was carried out on two isolated blocks of soil extracted from the field, representing the two typical forest types while excluding potential confounding factors, such as slope gradient, rainfall input heterogeneity, and slope orientation. The soil volume in isolated blocks, 300×100×50 cm^3 (projected length×width×height) with an inclination of 30°, was transferred by cutting boxes with the least disturbance to mimic field conditions. A 3 cm-thick drainage layer composed of gravels was placed between the soil volume and bedrock, serving as a widely recognized

https://doi.org/10.5194/egusphere-2025-1254
Preprint. Discussion started: 5 May 2025

soil-bedrock interface to facilitate lateral preferential flow in hillslopes (Graham and Lin, 2012). Both blocks were equipped with identical monitoring devices for water balance measurements (Fig. 1a), including soil water potential sensors and outflow gauges. Natural rainfall input was measured by tipping buckets deployed nearby. The monitored outflows included surface runoff, interflow, and subsurface flow (Fig. 1b). However, subsurface flow was the sole outflow observed during the entire monitoring period in both forests.

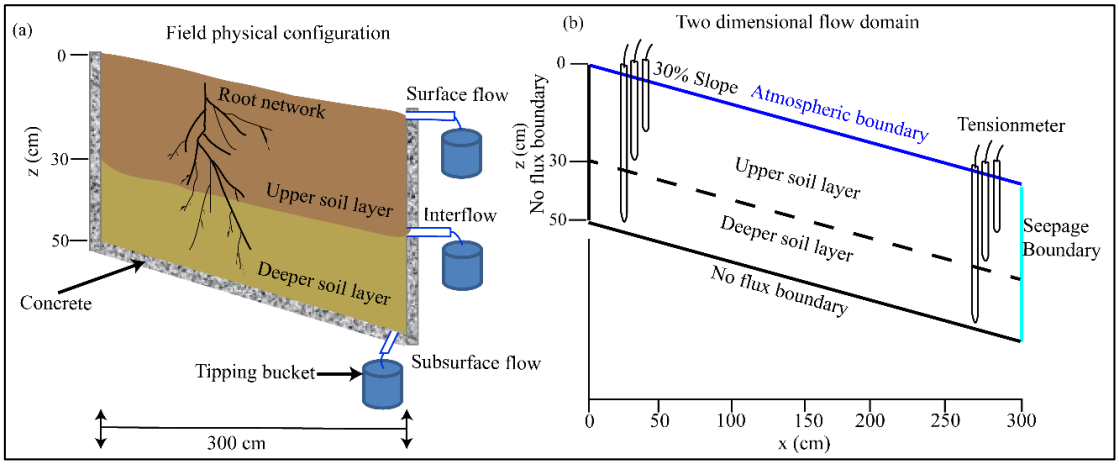

Figure 1: Artificial field configurations (a) and flow domain with boundary conditions in the numerical model (b).

2.2 Field experiments and previous researches

2.2.1 Field experiments on ground layer and soil

The interception capacity of the forest ground layer was obtained by simulated rainfall experiments on the artificial field configuration. Experiments of 150 mins duration, with simulated rainfall at constant intensity, were run at intensities of 5, 10, 20, and 40 mm hr^{-1}. Five groups of T4e sensors were distributed evenly along the hillslope for soil water storage calculation, then the interception capacity was calculated by the water balance equation.

To determine the saturated hydraulic conductivity of the soil matrix (K_{ms}), a tension infiltrometer called "hood infiltrometer" was used (Demand et al., 2019). For every measurement location infiltration rates with at least three tensions between 0.4 and 5.9 hPa were recorded, allowing us to fit an exponential function to calculate Kms at a tension of 6 hPa (Gardner, 1958). At this tension, pores with a diameter >0.5 mm are excluded from flow and measured hydraulic conductivity represent matrix infiltration capacities (Jarvis, 2007). However, due to the high macroporosity at many locations, adjusting the pressure in the hood was difficult, and measurements were only possible at tensions of 1–4 hPa. Therefore, for some sites, the Kms is an extrapolation of the Gardner fit to a tension of 6 hPa (Demand et al., 2019).

https://doi.org/10.5194/egusphere-2025-1254
Preprint. Discussion started: 5 May 2025

2.2.2 Previous researches on PFPs

Dye tracer experiments declared that prominent PFPs were in form of macropores within the root zone. Moreover, dye tracer experiments revealed that PFPs are well-connected in vertical direction, while PFPs are discrete in lateral direction (Wang et al., 2022). The mean transport distance of tracer at the lateral direction was around ~25 cm. It is believed that abundant root distribution, rock fragment, and coarse soil contributed to the connected flow paths at vertical direction within the root zone in both forests, this is also confirmed by a similar occurrence frequency of preferential flow in both forests. Intact soil cores (50 mm in diameter and height) were sampled and scanned to determine the macroporosity (ratio of pores with a diameter over 30 μm to the total soil column) in the root zone. The results showed that the macroporosity ranged between 3% and 16%, with a mean value of ~8% in the coniferous forest and ~9% in the broadleaf forest (personal communication, Yang et al., 2023).

2.3 Numerical modelling

2.3.1 Numerical model and mode set-up

The HYDRUS 2D is a physically based finite-element model for simulation of two-dimensional water movement in variably saturated media by numerically solving the Richards' equation (Šimůnek et al., 2016; Šimůnek et al., 2012). It allows us to explicitly represent different soil structures (i.e., PFPs and ground layer) and adjust their characteristics, facilitating our understanding of interplay between hillslope form and function.

An 2D flow model identical to the artificial field configuration was established (Fig. 1b). The model set-up included a constant 3 cm-thick soil-bedrock PFP. An initial discretization size of 5×5 mm for the cross-section of the hillslope was chosen to balance the necessary detail to represent PFPs and minimize computational cost (Fig. 2). A no flux boundary condition was imposed at the bottom bedrock boundary and up vertical boundary, while a seepage face boundary and an atmospheric boundary condition were specified at the lower vertical boundary and the soil surface, respectively (Fig. 1b).

The PFPs within the soil were conceptualized as the vertical connected PFPs (vPFPs) and lateral discrete PFPs (lPFPs) in the 2D cross-section according to previous knowledge. To represent the PFPs in the model, we applied a random placement method. Five different macroporosity were used for vPFPs: 3% for lower boundary intensity (Lb), 5% for low intensity (L), 10% for middle intensity (M), 15% for upper boundary intensity (Ub), 20% for out of boundary intensity (Ob). Half of these intensities were assigned to discrete lPFPs—1.5%, 2.5%, 5%, 7.5%, 10%—due to observed half-length of lPFPs compared to the vPFPs, to test the different set-ups on subsurface flow (Table 1). Since the explicit distribution of PFPs in soils is still unknown, they were generated by using random components. The starting points of the vPFPs were appointed by a Poisson process and extended stepwise into the soil to a specific length determined by a normal distribution with a mean of 45 cm and standard deviation of 5 cm. The lPFPs were generated similarly, with starting points randomly generated and extended down hillslopes to a length determined by a normal distribution with a mean of 25 cm and a standard deviation of 5 cm. To examine the role of ground layer on subsurface flow, it was optionally included in the topmost row of the 2D flow domain.

https://doi.org/10.5194/egusphere-2025-1254
Preprint. Discussion started: 5 May 2025

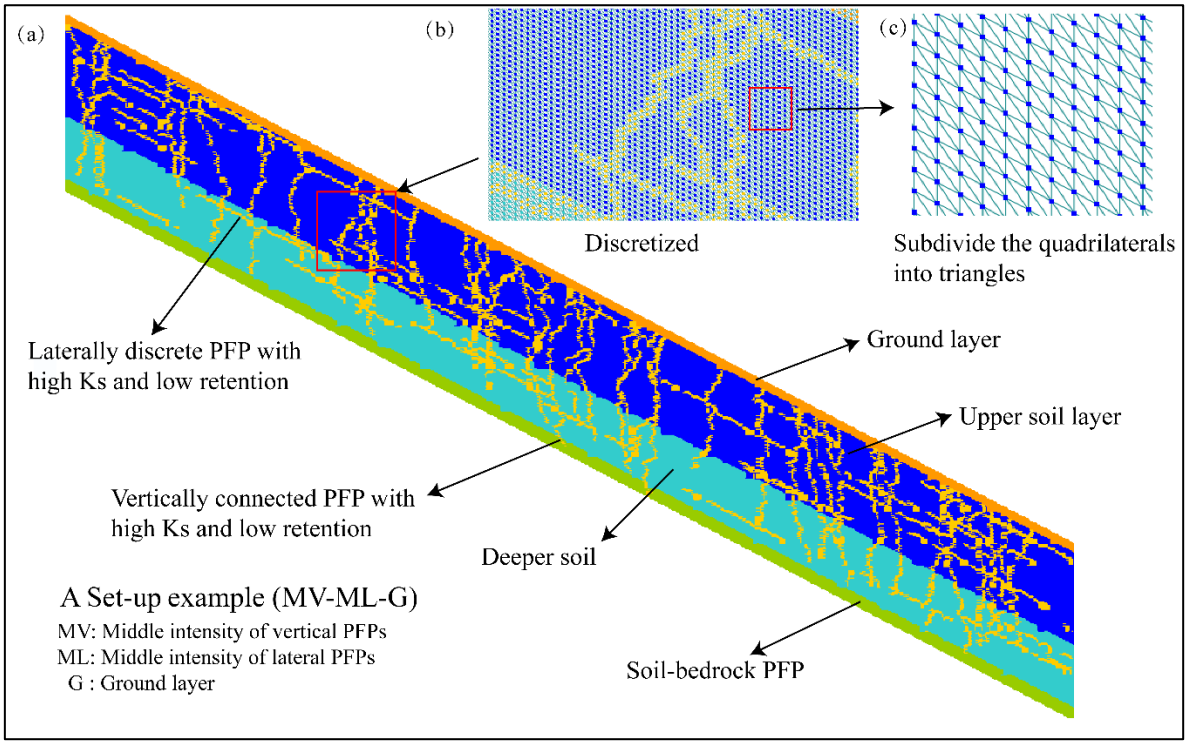

185 **Figure 2: A set-up of hillslope form with explicit structures (a) and discretization of the flow domain (b) in the numerical model.**

Table 1: Different types of structures and variants for numerical model set-up: four different types of structures.

Type of structures	Basic model variants and abbreviation
Ground layer	-thickness 3 cm -None
Vertically connected PFPs (length: 45± 5 cm normal distribution)	-Low boundary intensity 3%; LbV -Low intensity 5%; LV -Middle intensity 10%; MV -Upper boundary intensity 15%; UbV -Out of boundary intensity 20%; ObV
Laterally discrete PFPs (length: 25±5 cm normal distribution)	-Low boundary intensity 1.5%; LbL -Low intensity 2.5%; LL - Middle intensity 5%; ML -Upper boundary 7.5 %; UbL -Out of boundary intensity 10%; ObL
Soil-bedrock PFP (connected lateral PFP)	-thickness 3 cm

https://doi.org/10.5194/egusphere-2025-1254
Preprint. Discussion started: 5 May 2025

2.3.2 Mode parameters and evaluation

We assigned an effective porous medium with low retention properties to the meshes representing PFPs to minimize capillary forces. Partial parameters for PFPs were retrieved from a meta-analysis, applying a mean macropore flow velocity of 1.08×10^{-3} m s^{-1} (Gao et al., 2018). For the soil matrix, parameters were determined by multistep-outflow experiments on undisturbed soil columns under unsaturated conditions to exclude the hydraulic effects of macropores. The hydraulic properties of the different soil layers were modelled with a van Genuchten–Mualem parameterization (Table 2). The ground layer was likewise parameterized as a highly conductive medium with high porosity. The ground layer was treated as a "soil layer", and the residual "soil" water content was set at a high value, and the saturated "soil" water content was set as the sum of residual water content and equivalent interception capacity. The soil-bedrock interface was also conceptualized as a highly conductive medium with low retention capacity, akin to PFPs (Table 2).

To investigate the role of PFPs and the ground layer in subsurface flow, and to identify active PFPs involved in subsurface flow, we first performed a short time simulation of a typical rainfall event that represents local rainfall characteristics, simulation. This allowed us to examine how hillslope structure (i.e., PFPs and ground layer) affects subsurface flow and identify set-ups that meet evaluation criteria. We then performed a long time (i.e., growing season) simulation to reduce set-ups identified at event scale and identify the active PFPs involved in surface flow in both forests across different scales, because of equifinality. The simulated subsurface flow was compared with the observed flow, and set-ups were deemed acceptable if they met the following evaluation criteria: Nash-Sutcliffe Efficiency (NSE) greater than 0.75, root mean square error (RMSE) less than half of the standard deviation of subsurface flow, and matched the observed water balance by 10% (Wienhöfer and Zehe, 2014).

3 Results

3.1 Hillslope subsurface flow at even scale

The selected rainfall event lasted from 7 Jun 2020 17:00:00 to 11 Jun 17:00:00, spanning 97 hrs with multiple peaks and a mean intensity of 0.88 mm hr^{-1} (69 mm in total), which was close to the mean intensity of 0.85 mm hr^{-1} for the whole monitoring period. The subsurface flow ranged from 4.24 to 91.59 cm^2 hr^{-1}, with a standard deviation of 17.81 cm^2 hr^{-1} in the broadleaf forest, and from 4.40 to 77.92 cm^2 hr^{-1}, with a standard deviation of 15.69 cm^2 hr^{-1} in the coniferous forest.

Overall, the model evaluation criteria of 50 set-ups for each forest type were summarized (Table 3). A total of 36 setups in the coniferous forest and 39 set-ups in the broadleaf forest achieved an NSE higher than 0.75, with maximum NSE values of 0.86 and 0.88, respectively. Under LbV and LV, all set-ups with ground layer met NSE. However, as the intensity of vPFPs increased, the number of set-ups meeting NSE sharply decreased. Additionally, 31 set-ups in the coniferous forest and 35 set-ups in the broadleaf forest met the criterion of RMSE that was within half the standard deviation of observed subsurface flow. These set-ups displayed significant variability with no discernible patterns. Regarding the water balance criterion, 6

https://doi.org/10.5194/egusphere-2025-1254
Preprint. Discussion started: 5 May 2025

set-ups in the coniferous forest and 5 set-ups in the broadleaf forest matched the water balance within an error of ±10%, with minimum water balance errors of 0.52% and 2.12%, respectively. Notably, the set-ups meeting water balance were observed only under LbV and LV without the ground layer (Fig. 3). Eventually, only 3 set-ups in the coniferous forest and 2 set-ups in the broadleaf forest fulfilled all three criteria, specifically they were LV-LbL, LV-LL, LV-ML in the coniferous forest, and LV-LL and LV-ML in the broadleaf forest (Table 3).

The successful simulation of set-ups meeting all three evaluation criteria was displayed against observed hydrographs (Fig. 3). The results demonstrated that only partial PFPs were involved or active in the runoff processes in both forests. Additionally, none of these 5 set-ups included a ground layer. However, simulations incorporating a ground layer exhibited elevated NSE (mean value of 0.86 with ground layer vs 0.79 without ground layer) under the LV in the broadleaf forest, while no significant discrepancy in NSE (mean value of 0.81 with ground layer vs 0.82 without ground layer) was observed in the coniferous forest.

Without considering the ground layer, a relationship between PFPs and subsurface flow were shown (Fig. 4). The results showed that there were positive linear relationships between subsurface flow and the intensity of connected PFPs in both forests. The coniferous forest exhibited higher slopes across all set-ups, indicating a faster increase in subsurface flow due to changes in PFPs compared to the broadleaf forest (Fig. 3). For different intensity of lPFPs, the larger intensity of lPFPs was, the smaller of the effect of vPFPs on the subsurface flow (Fig. 3). Since the hydraulic conductivity of PFPs was a key factor controlling water flow and retrieved from a broad studies, a sensitivity analysis aiming to clarify the effect of saturated hydraulic conductivity of PFPs (Ks_pfps) on modelling results was conducted and we found an exponential relationship between Ks_pfps and NSE and the results demonstrated that the broadleaf forest was more sensitive to the macropore flow velocity in the range of 2.22×10^{-5} to 1.83×10^{-1} m s^{-1} (Fig. S2).

Table 2: Parameters for different structures in the numerical model.

Type of structures	Coniferous forest					Broadleaf forest				
	θ_s (-)	θ_r (-)	K_s (m s^{-1})	α (cm^{-1})	n (-)	θ_s (-)	θ_r (-)	K_s (m s^{-1})	α (cm^{-1})	n (-)
Ground layer	0.41	0.30	0.54×10^{-3}	0.04	1.70	0.43	0.30	0.54×10^{-3}	0.04	1.70
0–30 cm soil	0.65	0.18	1.30×10^{-5}	0.08	1.32	0.63	0.31	1.50×10^{-5}	0.14	1.37
30–50 cm soil	0.55	0.15	1.19×10^{-5}	0.11	1.20	0.55	0.23	1.31×10^{-5}	0.13	1.40
Vertical and lateral PFPs	0.50	0.30	1.08×10^{-3}	0.05	1.50	0.50	0.30	1.08×10^{-3}	0.05	1.50
Soil-bedrock PFPs	0.38	0.30	1.08×10^{-3}	0.05	1.50	0.38	0.30	1.08×10^{-3}	0.05	1.50

https://doi.org/10.5194/egusphere-2025-1254
Preprint. Discussion started: 5 May 2025

Table 3: Summary table of simulations under different set-ups in relation to the three model evaluation criteria ("N": NSE greater than 0.75; "R": RMSE less than half of standard deviation; and "W": water balance error less than 10%), letters indicate which criteria were fulfilled, and underlined and italic text indicate all criterion was fulfilled).

		Coniferous forest					Broadleaf forest				
		LbL※ (1.5%)	LL (3%)	ML (5%)	UbL (7.5%)	ObL (10%)	LbL (1.5%)	LL (3%)	ML (5%)	UbL (7.5%)	ObL (10%)
LbV (3%)	+ground layer	NR	NR	NR	NR	N	NR	NR	NR	NR	N
	-ground layer	W	W	W	NR	NR	W	W	—	NR	NR
LV (5%)	+ground layer	NR	NR	NR	NR	NR	NR	NR	NR	NR	NR
	-ground layer	***NRW***	***NRW***	***NRW***	NR	NR	W	***NRW***	***NRW***	—	NR
MV (10%)	+ground layer	NR	NR	NR	—	—	NR	NR	NR	N	N
	-ground layer	NR	NR	NR	NR	NR	NR	NR	NR	NR	NR
UbV (15%)	+ground layer	NR	—	—	—	—	NR	NR	NR	NR	—
	-ground layer	NR	NR	NR	NR	—	NR	NR	NR	—	NR
ObV (20%)	+ground layer	N	—	—	—	—	NR	NR	NR	—	—
	-ground layer	NR	NR	N	N	N	NR	NR	NR	NR	—

Note: "—" denotes NSE value less than 0.75.

※ The abbreviation of Lb, L, M, Ub, and Ob denote different intensity of preferential flow paths as follows: Lb (lower boundary intensity), L (low intensity), M (middle intensity), Ub (upper boundary intensity), and Ob (out of boundary intensity); the letter "L" and "V" after the intensity means the directions of preferential flow paths at lateral and vertical conditions, respectively.

https://doi.org/10.5194/egusphere-2025-1254
Preprint. Discussion started: 5 May 2025

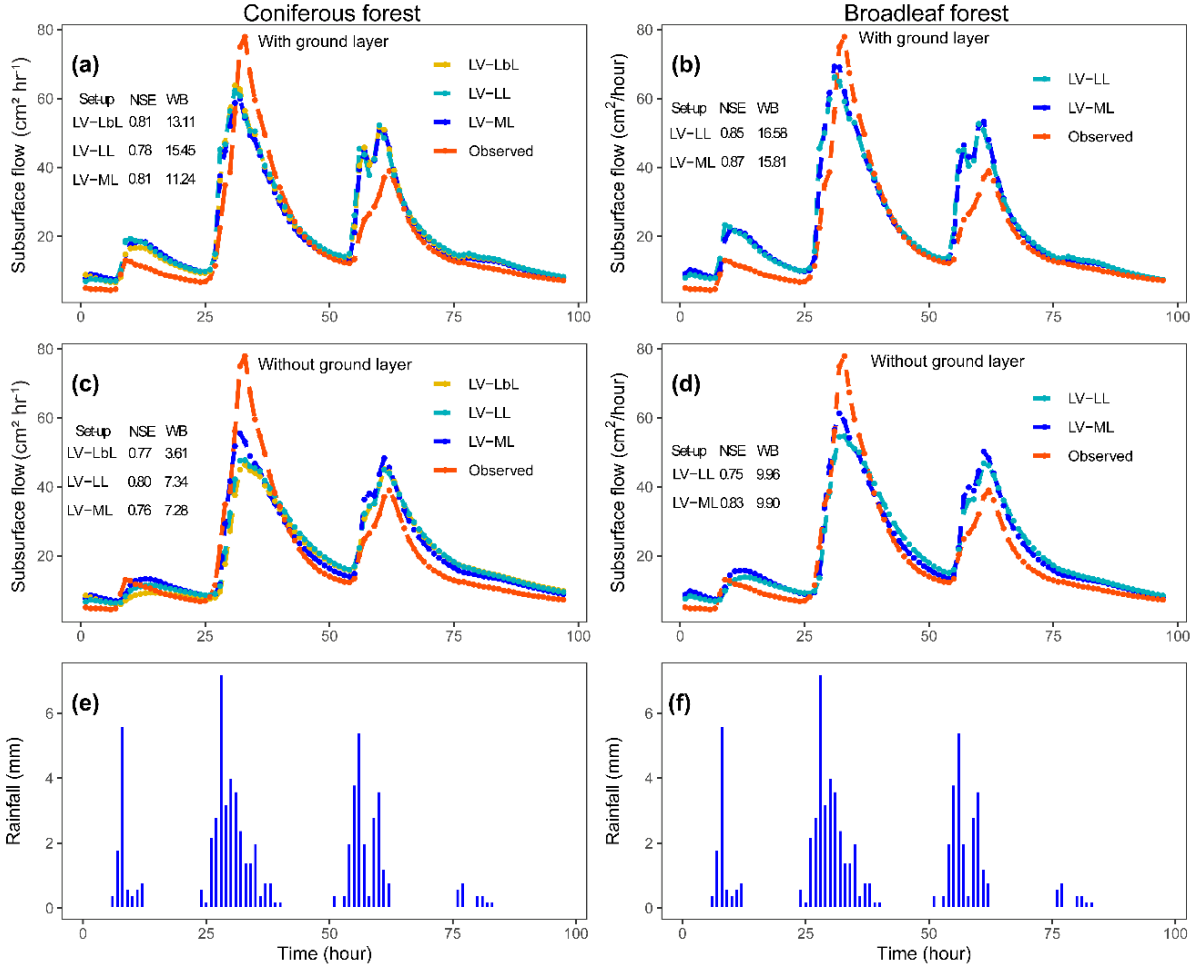

250 **Figure 3: Observed and simulated hydrographs of the acceptable set-ups in the coniferous forest (a, c) and broadleaf forest (b, d) at event scale (e, f).**

https://doi.org/10.5194/egusphere-2025-1254
Preprint. Discussion started: 5 May 2025

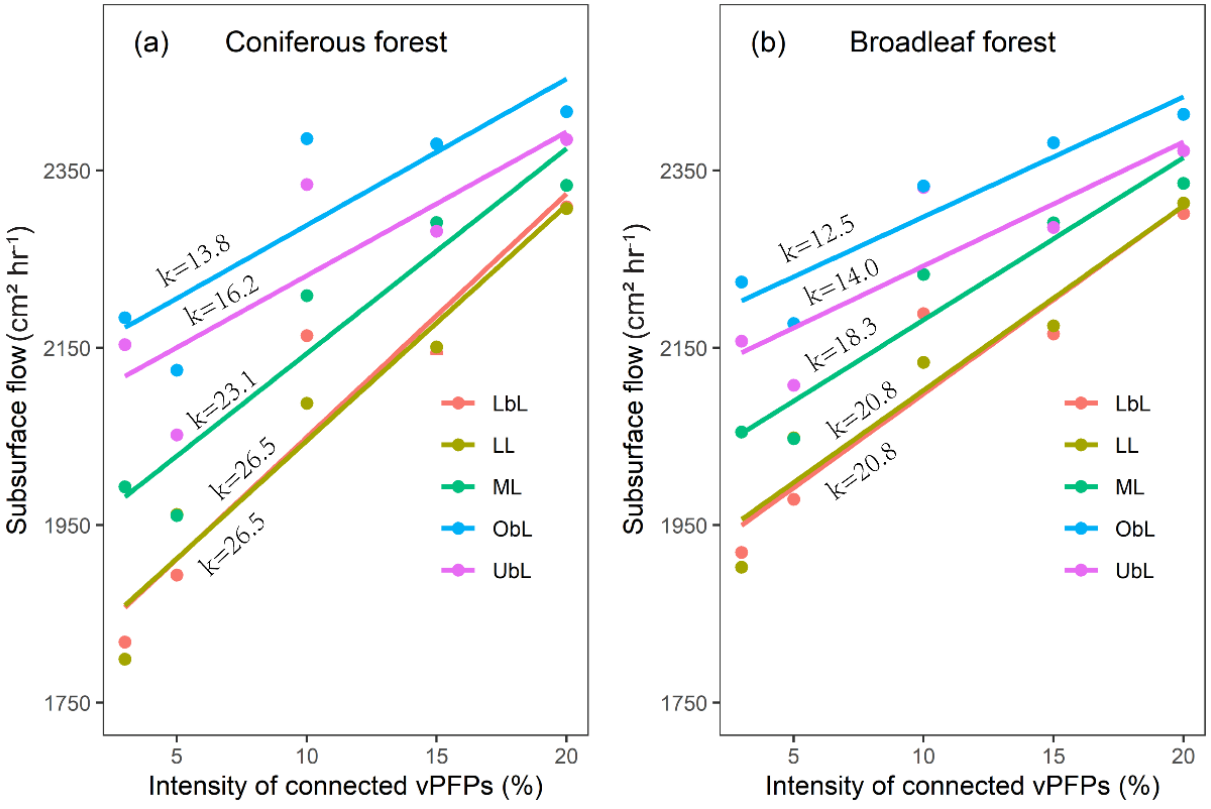

Figure 4: The relationships between the total subsurface flow and the intensity of connected vPFPs in the coniferous forest (a) and broadleaf forest (b).

3.2 Hillslope subsurface flow at seasonal scale

The simulation period at seasonal scale started from 23 May 2020 00:00:00 to 5 Oct 2020 16:00:00, resulting in a total time of 3257 hrs (~136 days) and rainfall amount of 1412.95 mm. Three and two set-ups that matched all model evaluation criteria at the event scale were directly used to simulate the long-term subsurface flow dynamics. The results showed a reduction in acceptable set-ups: from three to two in the coniferous forest and from two to one in the broadleaf forest. This indicated that long-term simulation reduced the number of acceptable set-ups, favouring the reduction in model equifinality and increasing the proximity of set-up to actual hillslope/soil structures. The final set-ups meeting all three evaluation criteria at seasonal scale were LV-ML (NSE = 0.83, RMSE = 6.06, and WB = 1.04%) and LV-LbL (NSE = 0.80, RMSE = 6.66, and WB = 0.95%) in the coniferous forest, and LV-ML (NSE = 0.80, RMSE = 6.59, and WB = 2.26%) in the broadleaf forest. The reduced set-up was LV-LL (NSE = 0.69, RMSE = 8.12, and WB = 1.17%) in the coniferous forest, and LV-LL (NSE = 0.74, RMSE = 7.47, and WB = 2.16%) in the broadleaf forest. The hydrographs of set-ups with the highest NSE were displayed (Fig. 5). Despite successfully reproducing subsurface flow during the growing season, there was an obvious

https://doi.org/10.5194/egusphere-2025-1254
Preprint. Discussion started: 5 May 2025

mismatch in peak subsurface flow following heavy rainfall events, particularly those continuous heavy rainfall events within a short time.

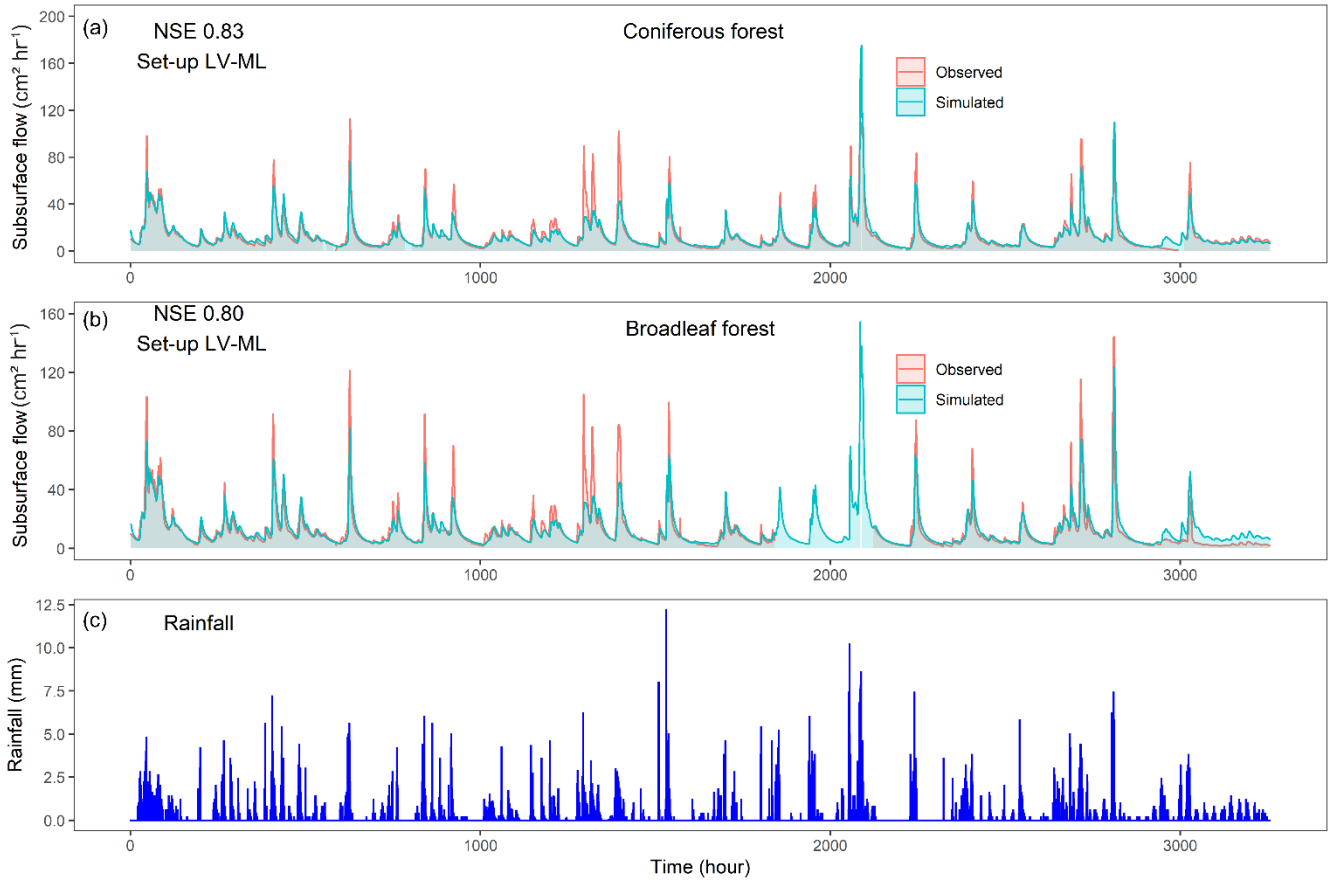

Figure 5: Observed and simulated hydrographs of the set-ups with the highest NSE in the coniferous forest (a) and broadleaf forest (b) during the growing season (c).

4 Discussion

4.1 Role of the ground layer in runoff processes

Forest ground layer significantly influenced the hillslope flow dynamics at event scale. Specifically, we found that the first simulated peak flow of set-ups with a ground layer achieved higher values and occurred later compared to those set-ups without a ground layer (Fig. 4; Table S1). Generally, the ground layer retains rainfall and delays water entry into PFPs, thereby delaying peak flow timing. In contrast, the set-ups without ground layer exhibited delayed peak flow timing. More PFPs received rainfall when directly connected to the atmosphere, leading to more water to be retained through the exchange between PFPs and soil matrix, thus we observed a consistently delayed occurrence of peak flow in both forest types (Fig. 4; Table S1). At the same time, the set-ups with ground layer demonstrated higher peak flow amount that was closer to the

https://doi.org/10.5194/egusphere-2025-1254
Preprint. Discussion started: 5 May 2025

observed values, aligning with the study showing that litter layer enhanced storm flood peak amount in short duration (Zhu et al., 2020). Owing to fast velocity of the ground layer, lateral flow within the ground layer leads to the rapid accumulation of downslope area and increase in soil moisture, resulting higher soil hydraulic conductivity. The process allows water to discharge more quickly and in greater amount, rather than being distributed thinly over the whole hillslope, as observed in set-ups without ground layer.

Besides, only the set-ups without a ground layer produced acceptable results, specifically the water balance error (Table 3). This is possibly ascribed to the rainfall characteristics and the hydraulic conductivity of the ground layer in our study area. The rainfall in this study is characterised by low intensity and long duration, decreasing water infiltration capacity into the soil through ground layer, thereby intensifying the lateral flow within the ground layer. Besides, the buried PFPs within soil is similar to that in agricultural fields where macropores started below the tilled topsoil (Akay and Fox, 2007; Holbak et al., 2021). However, a higher peak flow amount was observed in agricultural fields with buried macropores compared to surface-connected macropores, where the hydraulic conductivity of the "material" above macropores was 1.60 cm hr^{-1} (Akay and Fox, 2007) and 1.47 cm hr^{-1} (Holbak et al., 2021). These values are much less than that of the ground layer in this study, and their results were reached by column experiments under flat ground. Previous studies revealed that slope had negative effect on ground layer interception regardless of vegetation types, and lateral flow increased with the slope, particularly exceeding the threshold value of 15 degree (Zhao et al., 2022; Du et al., 2019). Therefore, the ground layer with high hydraulic conductivity and steep slope facilitates the lateral flow, resulting in better simulation results of set-ups without the ground layer at both the event and seasonal scales. Overall, this allows us to recognize the imperative of accounting for the ground layer by considering its hydraulic conductivity and lateral flow within it in addition to its interception capacity, particularly in many earth and hydrological models that ignore the ground layer or treat it as a simple bucket in runoff processes.

4.2 The PFPs involved in runoff processes in moraines

Previous studies revealed that the prevalence of bulk density decrease, clay-sized particles increase and organic matter accumulation in the long observation periods (over thousand years of soil development) of moraines over time. These factors are known to have impact on soil hydrology since they influence the soil structure (Hartmann et al., 2020a). In this study, glacial retreat in alpine mountains formed elevation-dependent moraines with primarily difference in temperature at elevation gradient. Soil development over time at lower elevation started earlier and experienced stronger weathering rate due to higher temperature, thus lower bulk density and less sand content was expected to be found in the broadleaf forest. However, the moraines are distributed along the valley with a mean slope of over 30 degrees, frequent precipitation and scouring carried away large amounts of fine particles at early bare and later vegetated phase of moraines, thus altering the traditional trend of clay accumulation (Li et al., 1986). This is also consistent with soil evolution model demonstrating that soil patterns become more heterogeneous due to increased tree throw and water erosion (Van Der Meij et al., 2020). Hence, coarse-textured soil with sand content over 85% was found in both forests. After the colonization of climax vegetation, plant

https://doi.org/10.5194/egusphere-2025-1254
Preprint. Discussion started: 5 May 2025

residues became the source of organic matter. The higher temperature in the broadleaf forest favoured plant residues decomposition and organic matter accumulation, leading to more soil particles coated with organic matter and resulting in higher residual soil water content and field capacity (Fig. S3). Thus, soil of the PFPs exhibited stronger soil suction at the same water content compared to the surrounding soil matrix, causing water to pool into PFPs and wet the surrounding soil matrix (Fig. S3). This process creates rapid and stable preferential flow once the surrounding soil matrix reaches its field capacity. Consequently, the coniferous forest is more sensitive to changes in PFPs compared to the broadleaf forest.

Land cover plays a key role in shaping hillslope internal structures, especially the number and type of PFPs (Guo and Lin, 2018; Benegas et al., 2014; Demand et al., 2019; Luo et al., 2010). In this study, the broadleaf forest, situated at a lower elevation with a higher average temperature, exhibited greater vegetation biomass and more animal activities than the coniferous forest. As a result, a larger number/intensity of macropores was found and expected to be involved in the runoff process in the broadleaf forest. However, modelling results contradicted this expectation, and set-ups with a low intensity of connected PFPs met evaluation criteria in both forests, manifesting that PFPs were only partially involved in the runoff process. The reasons for this come from several aspects. First, the connected PFPs may be mainly attributed to fine roots (< 2 mm in diameter). Studies have shown that the fine roots accounted for over 90% of roots in both deciduous broadleaf and evergreen coniferous forests and provided connected PFPs through an intensified interconnected network and void pores due to their fast turnover (Luo et al., 2019). Additionally, a consistent positive relationship between fine root density and subsurface flow has been found across different land covers (Nespoulous et al., 2019). In our study region, no significant difference in fine root content between forest types was found, with mean values of 77.5 ± 6.3 g kg^{-1} and 65.4 ± 7.6 g kg^{-1} in the broadleaf forest and coniferous forest, respectively (Xiong et al., 2024). Second, similar soil properties—including bulk density, soil porosity, soil texture, and rock fragments—were observed between forest types, primarily due to comparable rainfall pattern, which is recognized as the main factor influencing soil variation (Van Der Meij et al., 2020). Studies in moraines showed that only macropore flow via root channels was observed in deeper parts of soil in oldest moraine featured by prostrate shrubs together with small trees (Hartmann et al., 2020b). It further confirmed that PFPs are more related soil layering, organic matter content, root biomass, and root length density than soil texture by sprinkling experiments (Hartmann et al., 2022). These results are consistent with our previous study, which revealed a comparative preferential flow occurrence and runoff coefficient of shallow root zone, despite significant differences in root biomass between coniferous and broadleaf forests (Wang et al., 2022; Wang et al., 2024). This suggests that PFPs associated with fine roots rather than total macroporosity, should be the focus, as increased macroporosity or total root biomass does not necessarily enhance hillslope outflow.

Next, we explored the mechanism of preferential flow from a thermodynamic perspective, which provides insight into its nature. Although the prediction of onset, timing, and strength of preferential flow events remains challenging even when the PFPs in soil are known and identified. Zehe et al. (2010) and Lin (2010) introduced a novel thermodynamic viewpoint on preferential flow in soil, proposing that water flow organizes itself to maximize the dissipation of free energy—energy capable of performing work—for a given rainfall input, soil type, and soil structures. Since maximum reduction of free

https://doi.org/10.5194/egusphere-2025-1254
Preprint. Discussion started: 5 May 2025

energy brings the system closer to local thermodynamic equilibrium, enhancing mechanic stability by reducing hydro-mechanical stress and quickly alleviating mechanical and hydraulic loads (Zehe et al., 2013; Ehlers et al., 2011). In this study, the hydraulic conductivity of the soil matrix was found to be relatively higher (on the order of 10-5 m s-1), compared to the low rainfall intensity observed (Wang et al., 2022), and the persistent high soil moisture throughout the study period (Wang et al., 2023) indicates that the dissipation of free energy via surface flow is uncommon (Wang et al., 2024; Anderson et al., 2009; Angermann et al., 2017). Instead, water predominantly moves through PFPs, efficiently depleting free energy by facilitating the export of potential energy via subsurface flow, a primary form of free energy in wet soil (Zehe et al., 2013).This mechanism is consistent with the high frequency of preferential flow events previously observed in the study region (Wang et al., 2022).

A soil-mantled hillslope constitutes an open thermodynamic system that exchange mass, energy, and entropy with the surrounding to maintain the far from equilibrium, stable, and steady state (Zehe et al., 2013; Lin, 2010). This phenomenon promotes speculation that hillslope evolution may favour optimal structures, whereby materials with different properties are rearranged/arranged to maximize entropy production and energy dissipation across the system's boundary (Zehe et al., 2019; Lin, 2010). Overall, water flowing through the soil creates network-like flow paths in the subsurface and arrange soil properties—soil texture, soil layering, organic matter, soil structure, and other features—to reduce the flow resistance, thus forming a PF network that has the least global flow resistance (Lin, 2010). In the current study, the primary distinction between the two analysed hillslope arises from variation in solar radiation, which led to differing vegetation. While the amount, frequency, and intensity of rainfall input were similar for both sites, these conditions suggest that vegetation significantly influences hillslope structures, optimizing the depletion of free energy. Therefore, a close relationship exists between soil structures, specifically PFPs and vegetation, contributing to similar hillslope structures. This is consistent with research showing that the uncalibrated optimal density of macroporosity, derived by calculating the maximum reduction rates of free energy of soil water, enables long-term water balance simulation as well as the best fit when macroporosity was calibrated to match rainfall–runoff (Zehe et al., 2013; Zehe et al., 2019).

Schiavo (2023) studied preferential pathways of groundwater flow, inferred solely from geological data, using Gibbs' distribution and found these pathways likely evolve towards a zero-free energy state, demonstrating self-organization aimed at maximizing the reduction of free energy. Despite their propensity for rapid free energy reduction, the flow network formed by PFPs in soil do not always achieve the maximum local reduction of free energy. Studies have shown that only a limited number of particle paths pass through zones of high conductivity (e.g., PFPs) and connectivity in rapid PFPs network does not correlate with connected zones of continuously high hydraulic conductivity. In some cases, water particles emerge near vicinity of bottlenecks with low hydraulic conductivity since considerable energy is required to propel fluid through these restrictions, resulting in significant free energy depletion (Bianchi et al., 2011; Edery et al., 2014; Zehe et al., 2021; Bejan, 2007). This highlights how spatial variability in macroporosity only account for the localized maximum depletion of free energy, whereas water flow through a network of limited PFPs and the surrounding soil matrix facilitate the overall maximum depletion of free energy throughout the entire hillslope hydrological system.

https://doi.org/10.5194/egusphere-2025-1254
Preprint. Discussion started: 5 May 2025

4.3 Uncertainties and future outlooks

In the numerical model, we fixed parameters with some existing data to guide our conceptualization of PFPs and the ground layer. On the one hand, the parameters of ground layer were acquired through rainfall simulation, where the rainfall intensities were far larger than the mean rainfall intensity of the studied region. In addition, the ground layer was regarded as an isotopic layer, which may not accurately capture its distinct stratification, varying decomposition stages, and high spatial variability along hillslopes. Furthermore, the store and release dynamics of ground layer in response to rainfall input, which exhibit complex and unpredictable distinct phases (Guevara-Escobar et al., 2007; Du et al., 2019; Li et al., 2017), cannot be captured by a conventional "soil" water retention curve. On the other hand, the PFPs are deemed to represent macropores spanning the entire hillslope in forest soils, but other types of PFPs were not represented, such as observed finger flow in heterogeneous soils originated from moraines (Nimmo, 2021; Hartmann et al., 2020b; Hartmann et al., 2022). Besides, finger flow is controlled by pore-scale processes, for which the Richards' equation does not apply. Additionally, PFPs are emptied more rapidly, causing a lag in water content related to water potential, which do not follow a unique water retention curve as typically assumed when applying Richards equation (Vogel et al., 2023). In addition, the modelling approach by conceptualizing PFPs as explicit elements in the flow domain followed specific rules, therefore it cannot be ruled out that a more regular or irregular way would achieve better simulated results (Wienhöfer and Zehe, 2014).

In the generation of PFPs, the intensity of PFPs was retrieved from CT-imaged macropores, which were classified based on pore diameter exceeding certain threshold, through the threshold has not yet reached a consensus (Jarvis, 2007). We could retrieve an accurate intensity/number of PFPs if the macropores with diameter to what extent are governed by gravity force is known, thus leading to an improved simulation result. In the numerical model, the macropores network remained constant throughout the whole hydrological process, while the formation of connected PFPs through the self-organization of disconnect macropores depending on soil wetness is another aspect to consider (Sidle et al., 2001; Loritz et al., 2017; Nieber and Sidle, 2010). Nieber and Sidle (2010) showed that the preferential flow network expanded with the increasing degree of saturation, in which more macropores contributed to the flow. This non-stationary preferential flow network potentially explained the observed difference between simulated and observed subsurface flow peaks in this study (Fig. 4). For the long-term study, the changing input of mass and energy fluxes into the hydrological system, non-stationary configuration of the PFPs would persist due to varying vegetational structures, hydrothermal conditions, and soil wetness conditions, which contribute significantly to the change in macropores (Beven and Germann, 2013; Jarvis et al., 2016; Nimmo, 2021), thus confronting the challenge of depicting dynamic macropores network for a sound and accurate simulation is required in the future, particularly for floods prediction.

5 Conclusions

This study simulated subsurface flow using HYDRUS 2D, explicitly accounting for PFPs and ground layer in forested hillslopes developed from colonized valley moraines along an alpine mountain elevation, focusing on climax vegetation of

https://doi.org/10.5194/egusphere-2025-1254
Preprint. Discussion started: 5 May 2025

coniferous and broadleaf forests. The set-ups of hillslope form that successfully reproduce the field-observed hydrological responses were identified at event and seasonal scales, with the underlying mechanism explained from available field data and a thermodynamic perspective to emphasize the synergy between vegetations and soil properties.

The configuration of successful set-ups indicated that the intensity/number of vertically connected PFPs involved in the subsurface flow process were consistently low, representing 5% of total spatial area on both event and seasonal scales, in both coniferous and broadleaf forests. The low intensity of PFPs stems from the principle of least global flow resistance and maximum dissipation of free energy, achieved through water flow that combines partial PFPs with the soil matrix, rather than relying on all PFPs within the hillslope. The similar intensity of PFPs between forests was largely attributed to the similar coarse-texture soil resulting from frequent precipitation and washout of clay-sized particles, as well as comparable fine root content. The coniferous forest is more sensitive to changes in PFPs due to lower organic matter content in the soil profile. In addition, the ground layer significantly influences the subsurface flow by disconnecting PFPs with soil surface, decreasing peak flow in both forests. This study elucidated the feasibility of conceptualizing numerical models based on field evidence about PFPs and ground layer to successfully predict hillslope flow, and revealed the importance of vegetation (i.e., organic matter formation, fine roots, and ground layer) rather than soil properties (e.g., soil bulk density, texture, and rock fragments) in dominating water flow, advancing our knowledge in hillslope structures and runoff evolution over time in humid valley moraines.

Code availability

Codes that generated preferential flow paths through MATLAB 2020a is available upon request from the corresponding authors.

Data availability

Field monitoring data and the numerical modelling data are available upon request from the corresponding authors.

Author contributions

FW designed and carried out the analysis and wrote the original script. FW and RX. Y conducted the field and laboratory experiments. GX. W, JF. C, XY. T, JQ. D, and LG reviewed and edited the manuscript. XY. T and KW. H helped with the HYDRUS software and the modelling. GX. W and LG supervised the overall study as mentors.

Completing interests

The authors declare that they have no conflicts of interest.

https://doi.org/10.5194/egusphere-2025-1254
Preprint. Discussion started: 5 May 2025

Acknowledgements

This research was supported by the Science & Technology Fundamental Resources Investigation Program of China (Grant No. 2022FY100205) and the National Natural Science Foundation of China (Grant No. 42330508 & 42371039). We thank J. Wienhöfer (KIT University, Germany) and Mirek (PC-Progress, Czech Republic) for their kind reply to the technical issues.

References

Akay, O. and Fox, G. A.: Experimental Investigation of Direct Connectivity between Macropores and Subsurface Drains during Infiltration, Soil Sci. Soc. Am. J., 71, 1600-1606, doi:10.2136/sssaj2006.0359, 2007.

Anderson, A. E., Weiler, M., Alila, Y., and Hudson, R. O.: Subsurface flow velocities in a hillslope with lateral preferential flow, Water Resour. Res., 45, W11407, doi:10.1029/2008wr007121, 2009.

Angermann, L., Jackisch, C., Allroggen, N., Sprenger, M., Zehe, E., Tronicke, J., Weiler, M., and Blume, T.: Form and function in hillslope hydrology: characterization of subsurface flow based on response observations, Hydrol. Earth Syst. Sci., 21, 3727-3748, doi:10.5194/hess-21-3727-2017, 2017.

Bejan, A.: Constructal theory of pattern formation, Hydrol. Earth Syst. Sci., 11, 753-768, doi:10.5194/hess-11-753-2007, 2007.

Benegas, L., Ilstedt, U., Roupsard, O., Jones, J., and Malmer, A.: Effects of trees on infiltrability and preferential flow in two contrasting agroecosystems in Central America, Agric. Ecosyst. Environ., 183, 185-196, doi:10.1016/j.agee.2013.10.027, 2014.

Beven, K. and Germann, P.: Macropores and water flow in soils revisited, Water Resour. Res., 49, 3071-3092, doi:10.1002/wrcr.20156, 2013.

Bianchi, M., Zheng, C., Wilson, C., Tick, G. R., Liu, G., and Gorelick, S. M.: Spatial connectivity in a highly heterogeneous aquifer: From cores to preferential flow paths, Water Resour. Res., 47, W05524, doi:10.1029/2009wr008966, 2011.

Bogner, C., Mirzaei, M., Ruy, S., and Huwe, B.: Microtopography, water storage and flow patterns in a fine-textured soil under agricultural use, Hydrol. Processes, 27, 1797-1806, doi:10.1002/hyp.9337, 2013.

Cheng, Y., Ogden, F. L., and Zhu, J.: Earthworms and tree roots: A model study of the effect of preferential flow paths on runoff generation and groundwater recharge in steep, saprolitic, tropical lowland catchments, Water Resour. Res., 53, 5400-5419, doi:10.1002/2016wr020258, 2017.

Demand, D., Blume, T., and Weiler, M.: Spatio-temporal relevance and controls of preferential flow at the landscape scale, Hydrol. Earth Syst. Sci., 23, 4869-4889, doi:10.5194/hess-23-4869-2019, 2019.

Du, J., Niu, J., Gao, Z., Chen, X., Zhang, L., Li, X., van Doorn, N. S., Luo, Z., and Zhu, Z.: Effects of rainfall intensity and slope on interception and precipitation partitioning by forest litter layer, Catena, 172, 711-718, doi:10.1016/j.catena.2018.09.036, 2019.

Edery, Y., Guadagnini, A., Scher, H., and Berkowitz, B.: Origins of anomalous transport in heterogeneous media: Structural and dynamic controls, Water Resour. Res., 50, 1490-1505, doi:10.1002/2013WR015111, 2014.

Ehlers, W., Avci, O., and Markert, B.: Computation of Slope Movements Initiated by Rain–Induced Shear Bands in Small–Scale Tests and In Situ, Vadose Zone J., 10, 512-525, doi:10.2136/vzj2009.0156, 2011.

Gao, M., Li, H.-Y., Liu, D., Tang, J., Chen, X., Chen, X., Blöschl, G., and Ruby Leung, L.: Identifying the dominant controls on macropore flow velocity in soils: A meta-analysis, J. Hydrol., 567, 590-604, doi:10.1016/j.jhydrol.2018.10.044, 2018.

Gardner, W.: Some steady-state solutions of the unsaturated moisture flow equation with application to evaporation from a water table, Soil Sci., 85, 228-232, doi:10.1097/00010694-195804000-00006, 1958.

Gomyo, M. and Kuraji, K.: Effect of the litter layer on runoff and evapotranspiration using the paired watershed method, J. For. Res., 21, 306-313, doi:10.1007/s10310-016-0542-5, 2016.

Graham, C. B. and Lin, H.: Subsurface Flow Networks at the Hillslope Scale: Detection and Modelling, in: Hydropedology: Synergistic integration of soil science and hydrology, edited by: Lin, H., Academic Press, Waltham, MA, 559-593, 10.1016/b978-0-12-386941-8.00018-6, 2012.

https://doi.org/10.5194/egusphere-2025-1254
Preprint. Discussion started: 5 May 2025

Guevara-Escobar, A., Gonzalez-Sosa, E., Ramos-Salinas, M., and Hernandez-Delgado, G. D.: Experimental analysis of drainage and water storage of litter layers, Hydrol. Earth Syst. Sci., 11, 1703-1716, doi:10.5194/hess-11-1703-2007, 2007.
Guo, L. and Lin, H.: Chapter two - Addressing Two Bottlenecks to Advances the Understanding of Preferential Flow in Soils. In: Sparks, D.L. (Ed.), Advance in Agronomy., 10.1016/bs.agron.2017.10.002, 2018.
Hartmann, A. and Blume, T.: The Evolution of Hillslope Hydrology: Links Between Form, Function and the Underlying Control of Geology, Water Resour. Res., 60, e2023WR035937, doi:10.1029/2023wr035937, 2024.
Hartmann, A., Weiler, M., and Blume, T.: The impact of landscape evolution on soil physics: evolution of soil physical and hydraulic properties along two chronosequences of proglacial moraines, Earth Syst. Sci. Data, 12, 3189-3204, doi:10.5194/essd-12-3189-2020, 2020a.
Hartmann, A., Semenova, E., Weiler, M., and Blume, T.: Field observations of soil hydrological flow path evolution over 10 millennia, Hydrol. Earth Syst. Sci., 24, 3271-3288, doi:10.5194/hess-24-3271-2020, 2020b.
Hartmann, A., Weiler, M., Greinwald, K., and Blume, T.: Subsurface flow paths in a chronosequence of calcareous soils: impact of soil age and rainfall intensities on preferential flow occurrence, Hydrol. Earth Syst. Sci., 26, 4953-4974, doi:10.5194/hess-26-4953-2022, 2022.
Holbak, M., Abrahamsen, P., Hansen, S., and Diamantopoulos, E.: A Physically Based Model for Preferential Water Flow and Solute Transport in Drained Agricultural Fields, Water Resour. Res., 57, e2020WR027954, doi:10.1029/2020wr027954, 2021.
Hu, Z., Wang, G., Sun, X., Zhu, M., Song, C., Huang, K., and Chen, X.: Spatial-Temporal Patterns of Evapotranspiration Along an Elevation Gradient on Mount Gongga, Southwest China, Water Resour. Res., 54, 4180-4192, doi:10.1029/2018wr022645, 2018.
Huggett, R. J.: Soil chronosequences, soil development, and soil evolution: a critical review, Catena, 32, 155-172, doi:10.1016/S0341-8162(98)00053-8, 1998.
Jackisch, C., Angermann, L., Allroggen, N., Sprenger, M., Blume, T., Tronicke, J., and Zehe, E.: Form and function in hillslope hydrology: in situ imaging and characterization of flow-relevant structures, Hydrol. Earth Syst. Sci., 21, 3749-3775, doi:10.5194/hess-21-3749-2017, 2017.
Jarvis, N., Koestel, J., and Larsbo, M.: Understanding Preferential Flow in the Vadose Zone: Recent Advances and Future Prospects, Vadose Zone J., 15, 1-11, doi:10.2136/vzj2016.09.0075, 2016.
Jarvis, N., Coucheney, E., Lewan, E., Klöffel, T., Meurer, K. H. E., Keller, T., and Larsbo, M.: Interactions between soil structure dynamics, hydrological processes, and organic matter cycling: A new soil-crop model, Eur. J. Soil Sci., 75, e13455, doi:10.1111/ejss.13455, 2024.
Jarvis, N. J.: A review of non-equilibrium water flow and solute transport in soil macropores: principles, controlling factors and consequences for water quality, Eur. J. Soil Sci., 58, 523-546, doi:10.1111/j.1365-2389.2007.00915.x, 2007.
Kirchner, J. W., Benettin, P., and van Meerveld, I.: Instructive Surprises in the Hydrological Functioning of Landscapes, Annu. Rev. Earth Planet. Sci., 51, 277-299, doi:10.1146/annurev-earth-071822-100356, 2023.
Klaus, J. and Zehe, E.: A novel explicit approach to model bromide and pesticide transport in connected soil structures, Hydrol. Earth Syst. Sci., 15, 2127-2144, doi:10.5194/hess-15-2127-2011, 2011.
Koestel, J. and Larsbo, M.: Imaging and quantification of preferential solute transport in soil macropores, Water Resour. Res., 50, 4357-4378, doi:10.1002/2014wr015351, 2014.
Laine-Kaulio, H., Backnäs, S., Koivusalo, H., and Laurén, A.: Dye tracer visualization of flow patterns and pathways in glacial sandy till at a boreal forest hillslope, Geoderma, 259-260, 23-34, doi:10.1016/j.geoderma.2015.05.004, 2015.
Li, J., Zheng, B., Yang, X., Xie, Y., Zhang, L., Ma, Z., and Xu, S.: Glaciers in Tibet (in Chinese), Science Press, Beijing, China1986.
Li, X., Xiao, Q., Niu, J., Dymond, S., McPherson, E. G., van Doorn, N., Yu, X., Xie, B., Zhang, K., and Li, J.: Rainfall interception by tree crown and leaf litter: An interactive process, Hydrol. Processes, 31, 3533-3542, doi:10.1002/hyp.11275, 2017.
Lin, H.: Linking principles of soil formation and flow regimes, J. Hydrol., 393, 3-19, doi:10.1016/j.jhydrol.2010.02.013, 2010.
Loritz, R., Hassler, S. K., Jackisch, C., Allroggen, N., van Schaik, L., Wienhöfer, J., and Zehe, E.: Picturing and modeling catchments by representative hillslopes, Hydrol. Earth Syst. Sci., 21, 1225-1249, doi:10.5194/hess-21-1225-2017, 2017.

https://doi.org/10.5194/egusphere-2025-1254
Preprint. Discussion started: 5 May 2025

Luo, L., Lin, H., and Li, S.: Quantification of 3-D soil macropore networks in different soil types and land uses using computed tomography, J. Hydrol., 393, 53-64, doi:10.1016/j.jhydrol.2010.03.031, 2010.
Luo, Z., Niu, J., Xie, B., Zhang, L., Chen, X., Berndtsson, R., Du, J., Ao, J., Yang, L., and Zhu, S.: Influence of root distribution on preferential flow in deciduous and coniferous forest soils, Forests, 10, 986, doi:10.3390/f10110986, 2019.
Nespoulous, J., Merino-Martín, L., Monnier, Y., Bouchet, D. C., Ramel, M., Dombey, R., Viennois, G., Mao, Z., Zhang, J.-L., Cao, K.-F., Le Bissonnais, Y., Sidle, R. C., and Stokes, A.: Tropical forest structure and understorey determine subsurface flow through biopores formed by plant roots, Catena, 181, 104061, doi:10.1016/j.catena.2019.05.007, 2019.
Nieber, J. L. and Sidle, R. C.: How do disconnected macropores in sloping soils facilitate preferential flow?, Hydrol. Processes, 24, 1582-1594, doi:10.1002/hyp.7633, 2010.
Nimmo, J. R.: The processes of preferential flow in the unsaturated zone, Soil Sci. Soc. Am. J., 85, 1-27, doi:10.1002/saj2.20143, 2021.
Rasoulzadeh, A. and Homapoor Ghoorabjiri, M.: Comparing hydraulic properties of different forest floors, Hydrol. Processes, 28, 5122-5130, doi:10.1002/hyp.10006, 2013.
Sammartino, S., Lissy, A.-S., Bogner, C., Van Den Bogaert, R., Capowiez, Y., Ruy, S., and Cornu, S.: Identifying the functional macropore network related to preferential flow in structured soils, Vadose Zone J., 14, 1-16, doi:10.2136/vzj2015.05.0070, 2015.
Schiavo, M.: Entropy, fractality, and thermodynamics of groundwater pathways, J. Hydrol., 623, 129824, doi:10.1016/j.jhydrol.2023.129824, 2023.
Sidle, R. C., Noguchi, S., Tsuboyama, Y., and Laursen, K.: A conceptual model of preferential flow systems in forested hillslopes: evidence of self-organization, Hydrol. Processes, 15, 1675-1692, doi:10.1002/hyp.233, 2001.
Šimůnek, J., Genuchten, M. T., and Šejna, M.: Recent Developments and Applications of the HYDRUS Computer Software Packages, Vadose Zone J., 15, 1-25, doi:10.2136/vzj2016.04.0033, 2016.
Šimůnek, J., Van Genuchten, M. T., and Šejna, M.: HYDRUS: Model use, calibration, and validation, Trans. ASABE, 55, 1263-1274, doi:10.13031/2013.42239, 2012.
Šimůnek, J., Jarvis, N. J., van Genuchten, M. T., and Gärdenäs, A.: Review and comparison of models for describing non-equilibrium and preferential flow and transport in the vadose zone, J. Hydrol., 272, 14-35, doi:10.1016/S0022-1694(02)00252-4, 2003.
Sněhota, M., Císlerová, M., Amin, M. G., and Hall, L. D.: Tracing the Entrapped Air in Heterogeneous Soil by Means of Magnetic Resonance Imaging, Vadose Zone J., 9, 373-384, doi:10.2136/vzj2009.0103, 2010.
Uchida, T., Kosugi, K. i., and Mizuyama, T.: Effects of pipe flow and bedrock groundwater on runoff generation in a steep headwater catchment in Ashiu, central Japan, Water Resour. Res., 38, 24-21-24-14, doi:10.1029/2001wr000261, 2002.
van der Meij, W. M., Temme, A. J. A. M., Wallinga, J., and Sommer, M.: Modeling soil and landscape evolution – the effect of rainfall and land-use change on soil and landscape patterns, SOIL, 6, 337-358, doi:10.5194/soil-6-337-2020, 2020.
Vogel, H. J., Cousin, I., Ippisch, O., and Bastian, P.: The dominant role of structure for solute transport in soil: experimental evidence and modelling of structure and transport in a field experiment, Hydrol. Earth Syst. Sci., 10, 495-506, doi:10.5194/hess-10-495-2006, 2006.
Vogel, H. J., Gerke, H. H., Mietrach, R., Zahl, R., and Wöhling, T.: Soil hydraulic conductivity in the state of nonequilibrium, Vadose Zone J., 22, e20238, doi:10.1002/vzj2.20238, 2023.
Wang, F., Wang, G., Cui, J., Guo, L., Tang, X., Yang, R., and Huang, K.: Hillslope-scale variability of soil water potential over humid alpine forests: Unexpected high contribution of time-invariant component, J. Hydrol., 617, 129036, doi:10.1016/j.jhydrol.2022.129036, 2023.
Wang, F., Wang, G., Cui, J., Guo, L., Mello, C. R., Boyer, E. W., Tang, X., and Yang, Y.: Preferential flow patterns in forested hillslopes of east Tibetan Plateau revealed by dye tracing and soil moisture network, Eur. J. Soil Sci., 73, 13294, doi:10.1111/ejss.13294, 2022.
Wang, F., Wang, G., Cui, J., Guo, L., Tang, X., Yang, R., Du, J., and Sadegh Askari, M.: The nonlinear rainfall–quick flow relationships in a humid mountainous area: Roles of soil thickness and forest type, J. Hydrol., 641, 131854, doi:10.1016/j.jhydrol.2024.131854, 2024.
Wang, J., Pan, B., Zhang, G., Cui, H., Cao, B., and Geng, H.: Late Quaternary glacial chronology on the eastern slope of Gongga Mountain, eastern Tibetan Plateau, China, Sci. China Earth Sci., 56, 354-365, doi:10.1007/s11430-012-4514-0, 2012.

https://doi.org/10.5194/egusphere-2025-1254
Preprint. Discussion started: 5 May 2025

Weiler, M. and McDonnell, J. J.: Conceptualizing lateral preferential flow and flow networks and simulating the effects on gauged and ungauged hillslopes, Water Resour. Res., 43, W03403, doi:10.1029/2006wr004867, 2007.

Wienhöfer, J. and Zehe, E.: Predicting subsurface stormflow response of a forested hillslope – the role of connected flow paths, Hydrol. Earth Syst. Sci., 18, 121-138, doi:10.5194/hess-18-121-2014, 2014.

Wienhöfer, J., Germer, K., Lindenmaier, F., Färber, A., and Zehe, E.: Applied tracers for the observation of subsurface stormflow at the hillslope scale, Hydrol. Earth Syst. Sci., 13, 1145-1161, doi:10.5194/hess-13-1145-2009, 2009.

Xiong, J., Wang, G., Sun, X., Hu, Z., Li, Y., Sun, J., Zhang, W., and Sun, S.: Effects of litter and root inputs on soil CH4 uptake rates and associated microbial abundances in natural temperature subalpine forests, Sci. Total Environ., 912, 168730, doi:10.1016/j.scitotenv.2023.168730, 2024.

Zehe, E., Blume, T., and Bloschl, G.: The principle of 'maximum energy dissipation': a novel thermodynamic perspective on rapid water flow in connected soil structures, Phil. Trans. R. Soc. B, 365, 1377-1386, doi:10.1098/rstb.2009.0308, 2010.

Zehe, E., Loritz, R., Edery, Y., and Berkowitz, B.: Preferential pathways for fluid and solutes in heterogeneous groundwater systems: self-organization, entropy, work, Hydrol. Earth Syst. Sci., 25, 5337-5353, doi:10.5194/hess-25-5337-2021, 2021.

Zehe, E., Ehret, U., Blume, T., Kleidon, A., Scherer, U., and Westhoff, M.: A thermodynamic approach to link self-organization, preferential flow and rainfall–runoff behaviour, Hydrol. Earth Syst. Sci., 17, 4297-4322, doi:10.5194/hess-17-4297-2013, 2013.

Zehe, E., Loritz, R., Jackisch, C., Westhoff, M., Kleidon, A., Blume, T., Hassler, S. K., and Savenije, H. H.: Energy states of soil water – a thermodynamic perspective on soil water dynamics and storage-controlled streamflow generation in different landscapes, Hydrol. Earth Syst. Sci., 23, 971-987, doi:10.5194/hess-23-971-2019, 2019.

Zhao, L., Meng, P., Zhang, J., Zhang, J., Sun, S., and He, C.: Effect of slopes on rainfall interception by leaf litter under simulated rainfall conditions, Hydrol. Processes, 36, e14659, doi:10.1002/hyp.14659, 2022.

Zhu, H., Wang, G., Yinglan, A., and Liu, T.: Ecohydrological effects of litter cover on the hillslope-scale infiltration-runoff patterns for layered soil in forest ecosystem, Ecol. Eng., 155, 105930, doi:10.1016/j.ecoleng.2020.105930, 2020.